Object Detection with Sector Scanning Sonar

Jee Loong Chew and Mandar Chitre
Acoustic Research Laboratory, Tropical Marine Science Institute
National University of Singapore
18 Kent Ridge Road, Singapore 119227
Email: {jeeloong, mandar}@arl.nus.edu.sg

Abstract—The object detection subsystem is the foundation to object avoidance and path planning. It plays an active role in supporting the operations of an autonomous underwater vehicle (AUV). The first challenge with the implementation of an object detection subsystem for an AUV is in identification of a detection system. The considerations for implementing the sector scanning sonar over other acoustic and video imaging alternatives were based on the factors of its small size, lower power consumption, data rate and visibility. The next challenge is on achieving a reliable object detection subsystem. We review the Otsu thresholding and static thresholding for object detection using the sector scanning sonar. The proposed static thresholding is based on the methodology of an adaptive thresholding with constant false alarm rate (CFAR). Several modifications to the detection methodologies are proposed along with their advantages and disadvantages are also be presented. Experimental dataset collected at Republic of Singapore Yacht Club (RSYC) is used to evaluate the detection methodologies.

I. Introduction

The object detection subsystem plays a crucial role in supporting the operations of an autonomous underwater vehicle (AUV) and it is the foundation that leads to the object avoidance and path planning subsystems. Along with the command and control (C2) subsystem, it ensures the safety of the vehicle by detecting objects in the vicinity of the AUV. There are many challenges with the implementation of an object detection subsystem for an AUV. The first challenge is in identification of a detection system. Typically for an AUV, object detection can be achieved through acoustic and/or video imaging means. Acoustic sensing is more suitable for in-water operations as compared to video imaging sensing. This is primarily because sound waves can travel further in water, and thus it allows for further sensing range. There are various types of acoustic sensors, such as echosounder, sector scanning sonar, multibeam sonar and forward looking bathymetry sonar. In STARFISH AUVs [1], [2], the considerations for implementing the sector scanning sonar over a multibeam sonar are:

Data   The data output for a sector scanning sonar for each bearing ensonification is a 1—dimensional array, with its array size dependent on a configured range or resolution. A multibeam sonar typically yields readily interpretable images but at much higher data rate.

Size   The sector scanning sonar is more compact in terms of mechanical dimensions and integrates comfortably with the STARFISH AUV.

Power   The sector scanning sonar consumes less operating power.

The next challenge is on achieving a reliable object detection subsystem. The object detection subsystem typically consist of detection and representation methodologies. The detection methodology is responsible to process and analyze the sonar's data to determine whether an object is present or absent. The representation methodology is firstly used to localize the position of the AUV. Secondly, it is used to map and represent the environment.

II. Detection Methodology

In this section, we introduce detection methodologies based on Otsu thresholding and static thresholding. We discuss our approach to compute the static threshold based on the methodology of an adaptive thresholding with constant false alarm rate (CFAR). We also discuss our approach to compute the background statistics along with the consideration of annular statistics to determine the decision statistic.

A. Otsu Thresholding

Otsu thresholding [3] is a method that attempts to determine a threshold that can be used to discrimate the 2 modes. One of the mode represents the background data while the other mode represents the object(s). If a measurement exceeds the threshold, a binary decision can be made stating that an object is detected. Even if a measurement is marginally higher than the threshold, it would also result in it being considered an object. If the marginally higher measurement is from a valid object, then it is a valid positive detection. However, if the marginally higher measurement is not from a valid object, this can lead to undesired false alarm where non-valid object is considered as an object. False alarm can occur when measurement from the background environment is corrupted with noise.

The Otsu threshold is typically used as an image processing methodology [4]–[6] where several scanline measurements from a sector scanning sonar are collated and evaluated as a whole image. In terms of implementation, several adjacent and continuous scanline measurements firstly have to be collated to form a sectorial image before the threshold value is determined. The number of scanline measurements multiplied with the number of bins in each scanline measurement will be the required array size. The data output from a multibeam sonar would already be a 2—dimensional array image. This means that there will be a need for memory allocation such as an array to store the scanline measurements from a sector scanning sonar or the image output from a multibeam sonar.

B. Static Thresholding

In [7], the authors introduced an adaptive threshold implementation incorporating a constant false alarm rate (CFAR). The adaptive threshold Z is constructed based on the estimate of the background statistics, X_i, along with the number of background cells, N, and a threshold constant, K. The formulation of the adaptive threshold Z is as follows:

$$Z = K \sqrt{\frac{1}{N} \sum_{i=1}^{N} X_i^2} \tag{1}$$

The threshold constant K can be computed based on a desired probability of false alarm, P_{FA} as follows:

$$K = \sqrt{\left[(P_{FA})^{-\frac{1}{N}} - 1 \right] N} \tag{2}$$

The authors considered the background statistics, X_i, to be from neighbouring bins of the desired target bin and they are of similar heading or bearing. This is illustrated with the desired bin being the blue-colored grid while the neighbouring bins are the red-colored crosshatch dots as depicted in Fig. 1.
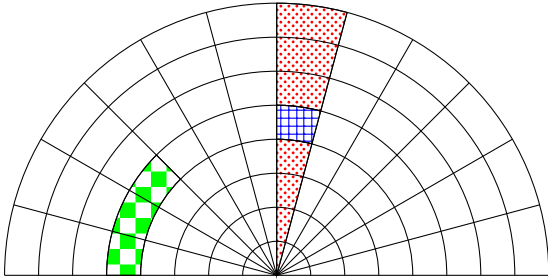

Fig. 1: Methodology to determine the background statistics X_i for adaptive thresholding

If we were to consider the neighbouring bins as the background statistics, it is assumed that the first order probability density function of the background statistics X_i to be Rayleigh distributed. Ideally, the neighbouring bins to the desired target bin should not contain any objects. If there is indeed an object in the desired target bin, it is assumed that the size of the object would only be contained within the desired target bin.

Assuming a Swerling III object model [7], [8], the authors also considered the detection probability to be a function of the average signal to noise ratio (SNR) of the desired target bin to the total noise power density from the background statistics X_i. The formulation for the detection probability P_D is as follows:

$$P_D = \left(\frac{\bar{X} + 2}{\bar{X} + 2 + \frac{2K^2}{N}} \right)^N \left[1 + \left[\frac{2K^2 \bar{X}}{(\bar{X} + 2)(\bar{X} + 2 + \frac{2K}{N})} \right] \right] \tag{3}$$

where

N	refers to the number of cells for each bin respectively in the background statistics
$\bar{X}$	refers to the average signal to noise ratio (SNR)

In this paper, we determine a threshold based on the adaptive thresholding methodology with some proposed modifications. Firstly, the background statistics X_i are based on an identified background sector and we consider annular statistics where the desired target will be compared with background statistics that are of similar bin or distance. This is illustrated with the desired bin being the blue-colored grid while the background bins are the green-colored checkerboard as depicted in Fig. 1. We believe annular statistics is more representative because scanline measurements of a similar bin or distance are attributed to similar propagation loss and processing gain. Besides that, we consider the median of the annular background statistics as the estimate of the background noise. We use the background noise estimate to normalize our decision statistic.

We did not solely rely on the adaptive threshold Z to determine a binary decision whether an object is indeed detected or not. We instead compute the probability of a target given a single measurement for position x, y, P_T and incorporate it into P_O. This allow us to make probabilistic statement of object detection. We propose that the probability of a target given a single measurement for position x, y, P_T to be similar to the formulation for the detection probability P_D as given in (3) with $\bar{X}$ being the decision statistic $\tilde{S}$. The advantage is that we will be able to compute the P_T of any target as a function of its detection statistic. P_T is defined as follows:

$$P_T = \left(\frac{\tilde{S} + 2}{\tilde{S} + 2 + \frac{2K^2}{N}} \right)^N \left[1 + \left[\frac{2K^2 \tilde{S}}{(\tilde{S} + 2)(\tilde{S} + 2 + \frac{2K}{N})} \right] \right] \tag{4}$$

where the decision statistic $\tilde{S}$ is the difference between measurement $s(\theta, i)$ and its respective background estimate $s_B(i)$ at bin i. It is defined as follows:

$$\tilde{S} = s(\theta, i) - s_B(i) \tag{5}$$

The background sector can be identified during the preparatory or calibration stage before the AUV executes the actual mission. Once we identified a background sector and are certain of the desired P_{FA}, the adaptive threshold Z and threshold constant K as given respectively in (1) and (2) can be pre-computed before the actual mission. The probability of a target given a single measurement for position x, y, P_T as given in (4) can also be pre-computed as a look-up table because we know that the bounds of the decision statistic $\tilde{S}$ is equivalent to the dynamic range of the measurement. The advantage is that there is no need to store the measurement as the analysis of the static thresholding can be made as soon as the measurement is acquired.

III. REPRESENTATION METHODOLOGY

An AUV subsystem for obstacle detection should include a means to map and represent the operating environment of the AUV. This can be done using occupancy grids [9] which represent map of the environment in an evenly spaced cell manner. The representation of the environment with grid cells is rather similar to how the elements in the scanline data represent spatial information. In each cell, information pertaining to occupancy is stored. Whenever a cell is ensonified by the sonar, its occupancy can be updated based on the cell's
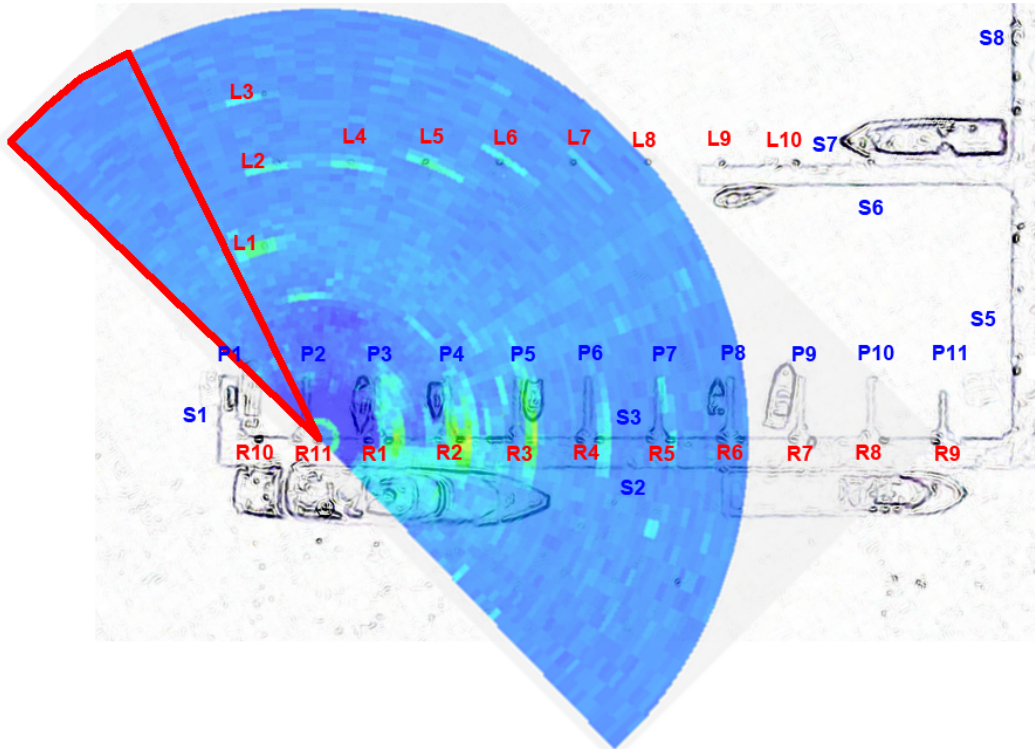
Fig. 2: Overlay of median statistics of the scanline measurements image with satellite view of potential targets at RSYC. A background sector to the portside of the sonar can identified by the red triangle.

object detection methodology. There are many formulations for the occupancy grid. In this paper, we adopt the formulation of the log-odds ratio described in [10]. It is briefly presented as follows:

$$
\begin{aligned}
l_{x,y}^{(t)} &= \log \frac{P(m_{x,y}|s_{x,y}^{(1:t)})}{1 - P(m_{x,y}|s_{x,y}^{(1:t)})} \\
&= \log \frac{P(m_{x,y}|s_{x,y}^{(t)})}{1 - P(m_{x,y}|s_{x,y}^{(t)})} + \log \frac{1 - P(m_{x,y})}{P(m_{x,y})} + l_{x,y}^{(t-1)}
\end{aligned}
$$
(6)

where

$l_{x,y}^{(t)}$	refers to the log-odds ratio of $P(m_{x,y}|s_{x,y}^{(1:t)})$ at timestep t
$s_{x,y}^{(t)}$	refers to the scanline measurement for position x, y at timestep t
$s_{x,y}^{(1:t)}$	refers to the scanline measurements for position x, y from timestep 1 to t
$P(m_{x,y})$	refers to the probability of occupancy. It is typically set to a value of 0.5 that translates to a 50% chance of a grid cell being occupied.
$P(m_{x,y}|s_{x,y}^{(t)})$	refers to the probability of occupancy given the current scanline measurement for position x, y. We propose to relate it with P_T as given in (4).
$P(m_{x,y}|s_{x,y}^{(1:t)})$	refers to the probability of occupancy at position x, y conditional on the scanline measurements from timestep 1 to t.

We term it the probability of an object present P_O.

$l_{x,y}^{(t-1)}$ refers to the log-odds ratio of the prior timestep $t-1$

The initialization, $l_{x,y}^{(0)}$, is generally set as:

$$
l_{x,y}^{(0)} = \log \frac{P(m_{x,y})}{1 - P(m_{x,y})}
$$
(7)

IV. EXPERIMENTAL RESULT — STATIC SETUP AT RSYC

An experiment with the Micron DST sonar [11] was conducted at Republic of Singapore Yacht Club (RSYC) to investigate its scanline statistics of targets detection. An overlay of a sonar image on the satellite view of the potential targets can be seen in Fig. 2. Targets with a prefix 'S' are ships/vessels that are present at the marina during the experiment. These are not targets intended to be ensonified. However, the draft and bottom-hull of these vessels might be ensonified and might appear as significant targets in the scanline measurements. Targets with a prefix 'P' are pier structures at the marina. Upon closer inspection, these pier structures are of floating structures and should not appear as significant targets in the scanline measurements. In addition to note are that these pier structures are actually supported by rigid columns labelled with prefixes 'L' and 'R'. The targets with a prefix 'L' and 'R' are respectively to the portside and starboard of the sector scanning sonar. These are the identified targets that should easily be ensonified and appear as significant targets in the scanline measurements.

A. Scanline Statistics

Firstly, we study the statistics of the background noise that are free of targets. We can identify the sector to the left of the sonar image as a suitable sample dataset. The background sector can be identified by the red triangle in Fig. 2. The mean and median of the background statistics along with the estimated Time Varying Gain (TVG) are presented in Fig. 3.
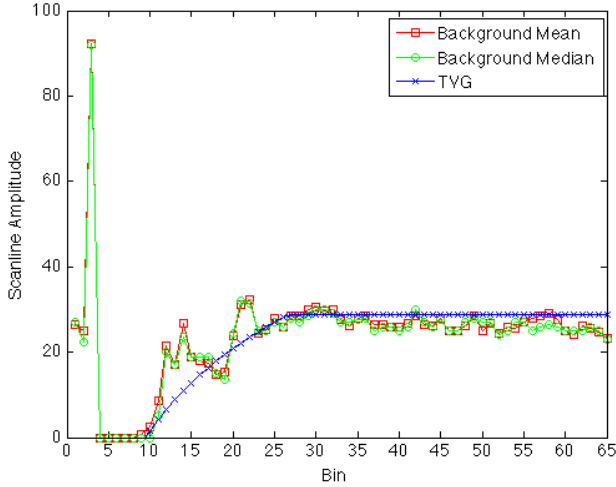

Fig. 3: Background statistics of the RSYC dataset along with the estimated TVG

TVG is a compensating gain that attempts to ensure the same echo level from an object regardless of its distance from the sonar. This is because the echo level of an object will suffer from 2-way propagation loss. The Micron DST sonar internally applies the TVG on the received signal. Therefore, the scanline measurements made available to the user are already compensated with TVG. We estimate the TVG because the actual values aren't made publicly available by the manufacturer. The estimation was made based on a restricted datasheet that contains some information about the sonar's internal processing gain. If the identified sector is indeed free of any targets, its scanline measurements would adhere to the estimated TVG. In Fig. 3, a spike corresponding to the transmission of the sonar ping can be observed at bin 3. The scanline amplitude is gradually increasing from bin 9 until bin 30. After bin 30, the background statistics is rather constant throughout. There are also some spikes observed between bin 12 to 15. These are indications that there are potential objects in those bins or there are higher intensity returns from the noise clutter. Otherwise, the mean and median of the background statistics can be observed to adhere closely to the estimated TVG.

The measurements of the targets are presented in Fig. 4. There are fluctutations observed in the intensity of the measurements. If the measurement fluctuates lower towards the background noise level, this can result in missed detection where an object is considered not being detected. If the measurement fluctuates higher, false alarm can occur where a non-object is being considered to be detected.
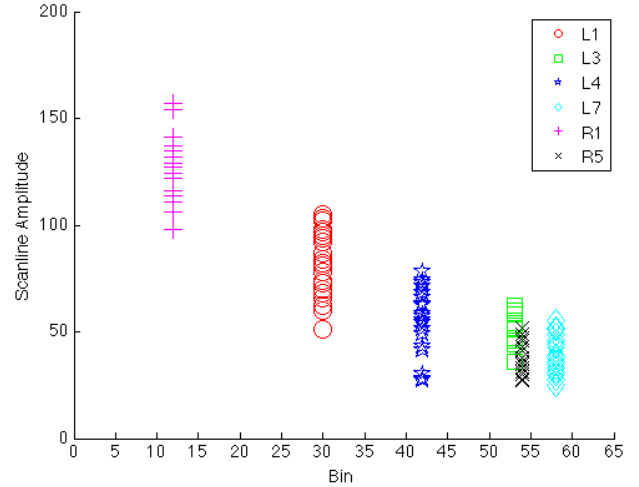

Fig. 4: Scanline measurements of the targets at RSYC

The detection statistic of the targets against the median background noise is presented in Fig. 5. L1 and R1 are targets that are less than 40m away with median detection statistic of more than 60. These targets are expected to have high P_T. L3 and L4 are targets with median detection statistic of 25. The detection statistic for L7 and R5 are less than 30 with a median of 10. R5 has several detection statistic nearing and at 0 while L4 and L7 have several negative detection statistic. This is because we were conservative when we considered the median background statistics as the background estimate. L3 and R5 are almost at the same distance but the decision statistic for L3 is slightly higher than R5. This means that L3 is likely to have higher P_T than R5. Besides that, the fluctuations for L4 encompasses the fluctuations for R5. However, most of the detection statistic for L4 is more than 25 but it is mostly less than 25 for R5. This means that L4 is still likely to have higher P_T than R5. Since L4 have several negative detection statistic, L4 might have lower P_T than R5 if the last few remaining detection statistic near 0 or becomes negative.
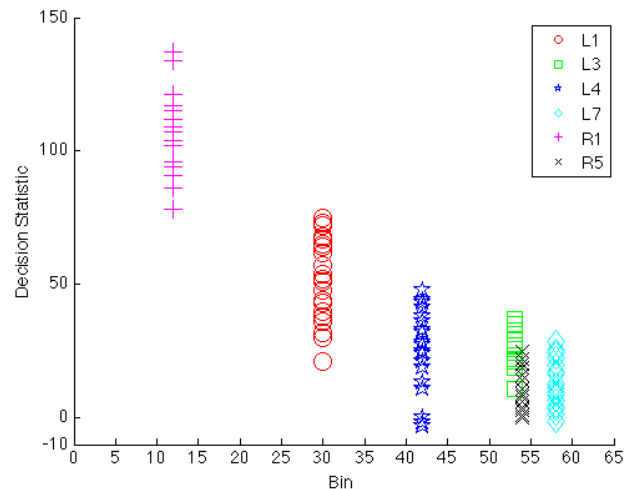

Fig. 5: Detection statistic of the targets at RSYC

B. Static Thresholding

Based on the background sector's scanline measurements identified in Fig. 2 and assuming the constant false alarm rate, P_{FA}, is set for 1% with the number of background statistics, N, as 8, the threshold constant K as given in (2) can be computed as 2.4952. The probability of a target given a single measurement for position x, y, P_T as given in (4) can then be computed as in Fig. 6. In Fig. 6, we observe that the increase of P_T is logarithmic with the increase of the detection statistic. The rate P_T increases is more significant when the detection statistic is between 0 and 20. The rate of increase is less when the decision statistic is from 20 till 40. After a detection statistic of 40, the rate increase is even slower. However, P_T is already reaching 70% probability.
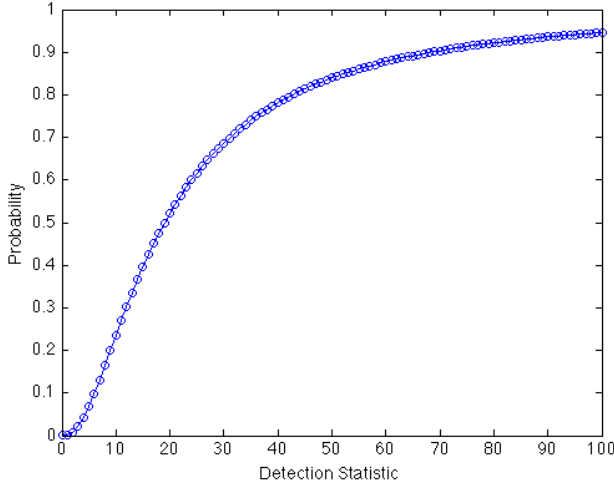
Fig. 6: Probability of a target given a single measurement for position x, y, P_T, based on a CFAR of 1%

Based on the detection statistic of the targets in Fig. 5, P_T for the targets can be computed as in Fig. 7.
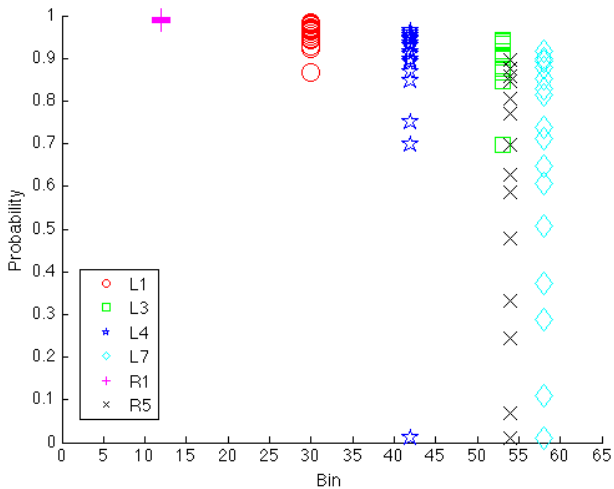

Fig. 7: Statistics of P_T of the targets at RSYC

It can be observed that R1 has high P_T with very low variations. All other targets have higher variations especially for L4, L7 and R5 that have P_T between 0 and 0.95. If a significant portion are of high probabilities, the targets should still be easily detected as the resulting P_O will be high. L1, L3 and L4 should have high P_O as their P_T are mostly higher than 0.6. R5 and L7 might have median P_O as their P_T are spread out between 0 and 0.9. The result of the occupancy grid can be seen in Fig. 8b. The result based on the static thresholding is able to detect all the identified targets as compared to the result using Otsu thresholding that is unable to detect that are farther way. The drawback with the static thresholding is that artifacts are detected to the starboard of the sonar. However, these artifacts also correspond to the high intensity scanline measurements observed in Fig. 2. An overview of the detection statistic, P_T and P_O for several of the targets are presented in Fig. 9. The observations are as follows:

L1   The detection statistic average more than 50. This results in P_T exceeding 80% and P_O remains high throughout.

L3   The detection statistic gradually increases nearing 40 and eventually fluctuates around 30. P_O gradually increases and remains high throughout.

L4   The detection statistic initially increases but there was a sudden decrease. The decrease resulted in very low P_T. After the 10th measurement, the detection statistic gradually increases nearing 40. P_T and P_O eventually became high.

L7   The detection statistic range from marginally near 0 to 30. Several of the initial decision statistic were close to 20 and these resulted in P_T of more than 80%. P_O remained high throughout because there were subsequent decision statistic that results in high P_T.

R1   The detection statistic throughout was with a median of 100. P_T and P_O remain high throughout.

R5   The detection statistic fluctuates between 0 and 25. After the 18th measurement, the decision statistic was slowly increasing. These result in several high P_T and P_O eventually became high.

P_T fluctuates accordingly with the detection statistic. P_T is amplified logarithmically when the increase of the detection statisic. However, a single increase of P_T doesn't immediately increases P_O. This can be observed for target L4 from the 7th measurement till the 9th measurement and also for target L7 that have several increases of P_T. P_O only increases if there are several continuously increasing P_T. This can be observed for target L4 from the 10th measurement onwards and also for target R5 from the 5th measurement till 7th measurement.
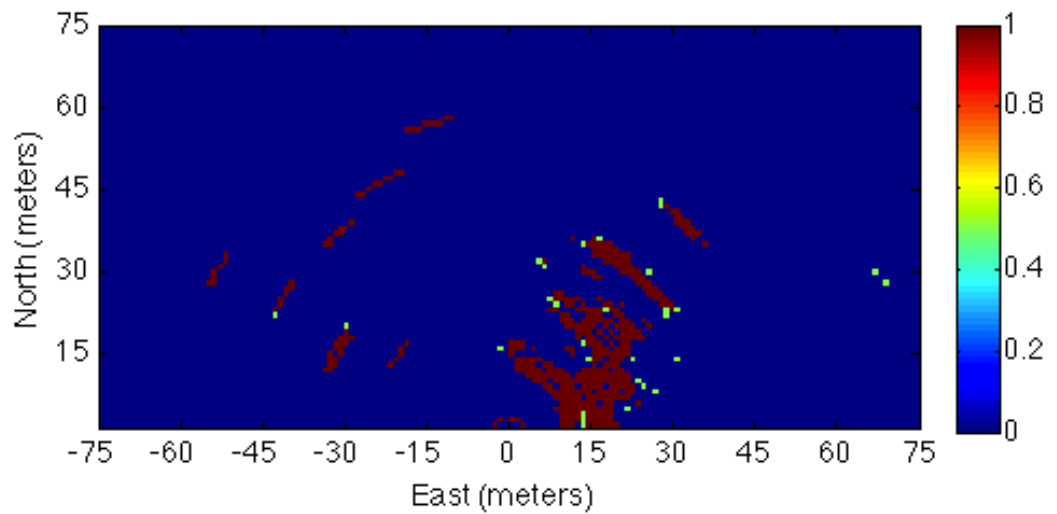
C. Otsu Thresholding

The result of Otsu thresholding in Fig. 8c was obtained based of the median statistics of the grid cell over 18 iterations with the threshold varying between 40 and 51. Each iteration has a field of view of 90° that was made of 30 scanline measurements. Targets L7 and R5 that are farther away from the sonar are not detected using Otsu thresholding but they are detected using the static thresholding. All other targets are easily detected. The Otsu thresholding is a lot of cleaner compared to the result using the static thresholding.
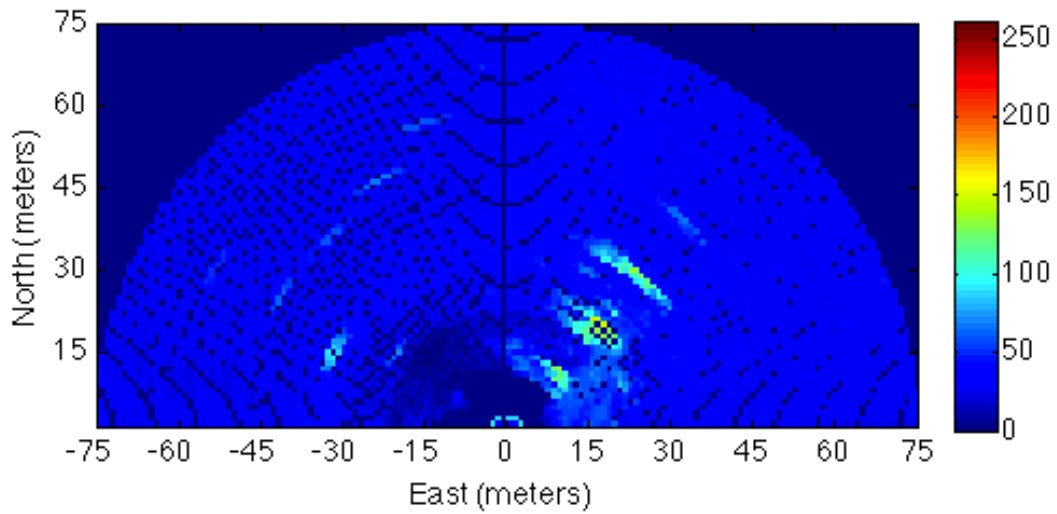
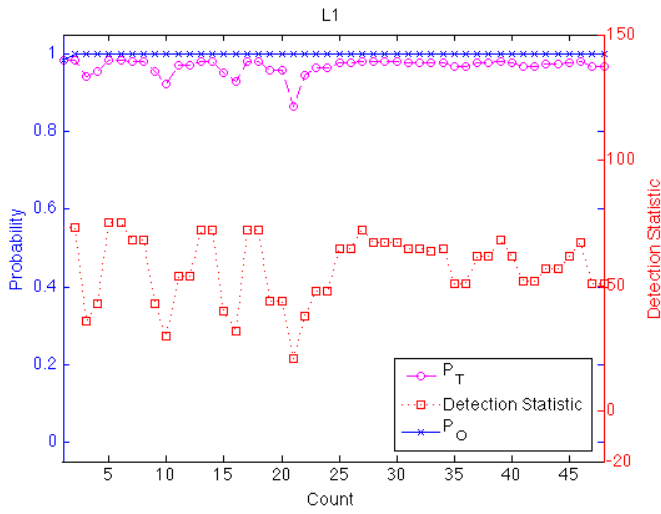(a) Median scanline statistics
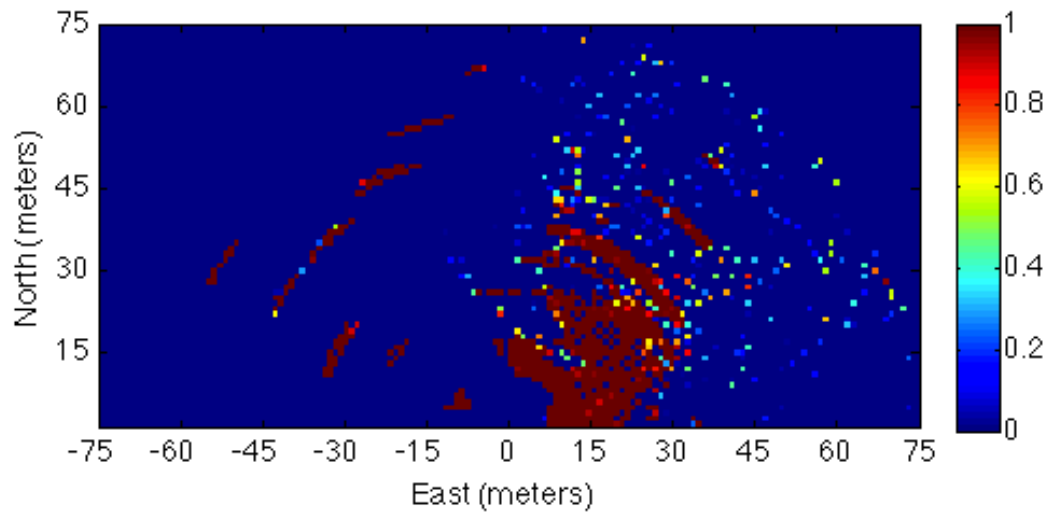
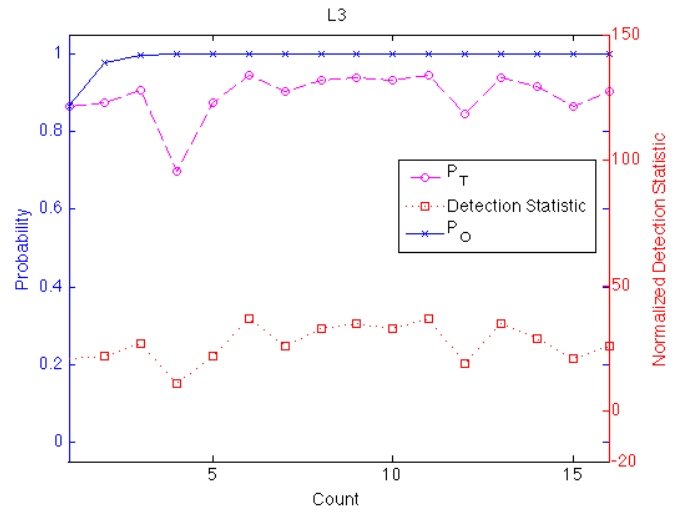(b) Result of object detection with static thresholding incorporating CFAR of 1%

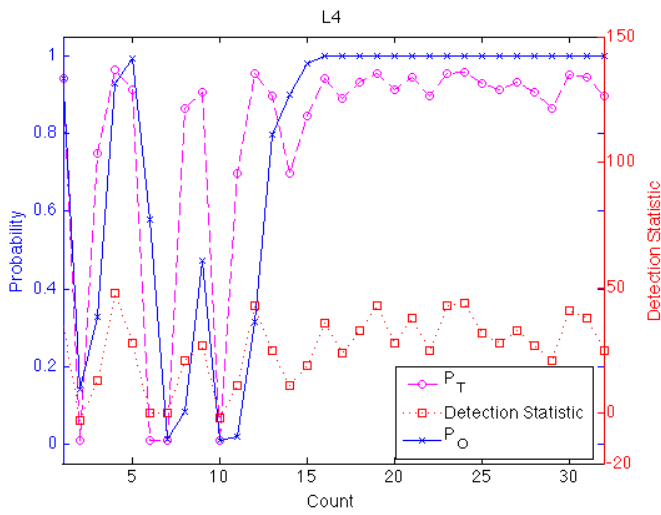(c) Result of object detection with Otsu thresholding on a sector of scanline measurements

Fig. 8: Median scanline statistics along with the results of Otsu thresholding and static thresholding for the RSYC dataset
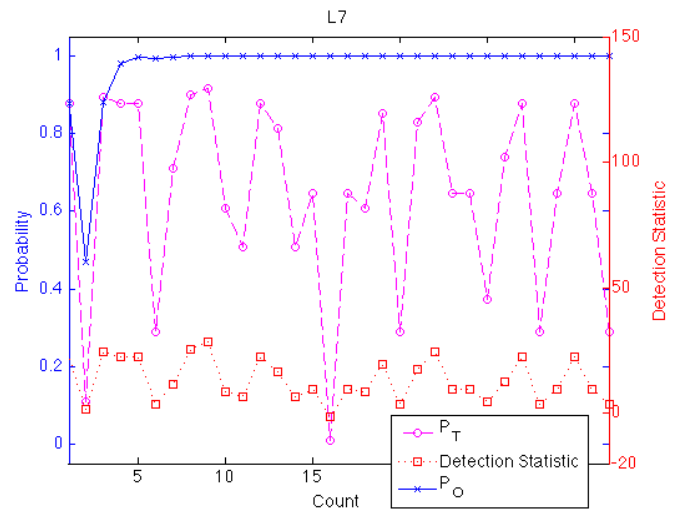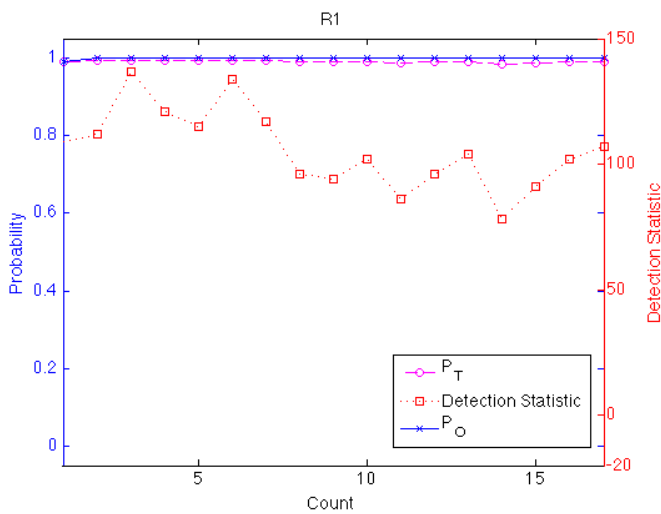
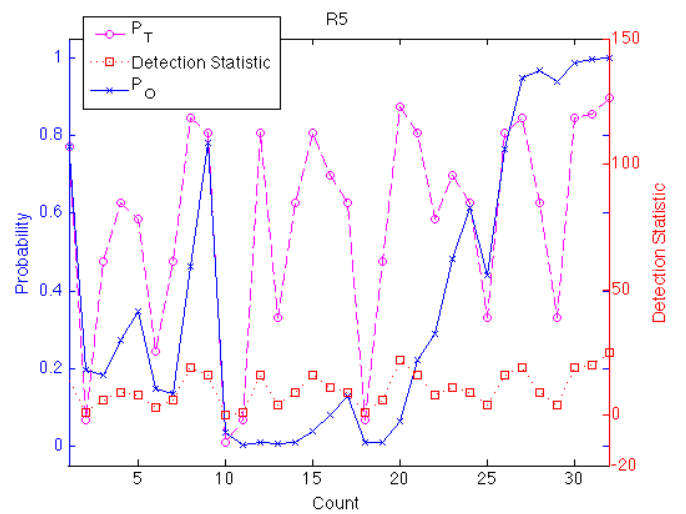Fig. 9: An overview of the detection statistic, P_T and P_O of the targets at RSYC

V. Conclusion

In this paper, we made several proposals to the adaptive thresholding methodology to estimate a static threshold that could be used for object detection during the AUV mission run. The first proposal is that a background sector can be identified during the preparatory stage of an AUV mission to allow us to determine the background statistics. This will allow us to pre-compute the annular background statistics before the actual mission run. The second proposal is that the decision statistic can be determined from the scanline measurement against its respective annular background statistics. Since the computation of probability of a target given a single measurement for position x, y, P_T is a function of the decision statistic, it can also be computed during the preparatory stage. Thus, P_T can easily be determined through a pre-computed look-up table during an actual mission run. Another advantage is that there is no need to store the measurements.

We also implemented the occupancy grid as a representation methodology coupled with a constant false alarm rate static threshold as the detection methodology. Occupancy grid was used to represent map of the environment in an evenly spaced cell manner. In each cell, information pertaining to occupancy was stored. We proposed to relate the probability of a target given a single measurement for position x, y, P_T to P_O which is also known as the probability of occupancy given the current measurement for position x, y, $P(m_{x,y}|s_{x,y}^{(t)})$. Thus, as measurements are attained, P_O can be updated based on P_T.

Finally, we presented the results of object detection using Otsu thresholding and static thresholding on an experimental dataset conducted at RSYC. Both approaches were able to detect all the targets except for Otsu thresholding that was unable to detect L7 and R5 that are farther away with measurements marginally near the background noise level. There were artifacts observed in the starboard of the sonar using static thresholding. However, this was consistent with the statistics of the actual measurements.

The Otsu thresholding methodology would require several scanline measurements to be collated before the binary detection result can be attained. The static thresholding methodology allows for the detection likelihood to be computed immediately when the measurements are acquired. We found out that P_T was a function of the detection statistic. This implied that the higher a scanline measurement is against its respective background statistics, the higher the probability of P_T would be. Probabilistic statements of detection can then be achieved when we incorporate P_T into the occupancy grid. In the result obtained through the static thresholding methodology, we observed that P_O only increases if there are several continuously increasing P_T. P_O would not be perturbed by a spurious P_T or detection statistic.

Acknowledgment

References

[1] T. B. Koay, Y. T. Tan, Y. H. Eng, R. Gao, M. Chitre, J. Chew., N. Chandhavarkar, R. Khan, T. Taher, and J. Koh, "Starfish - a small team of autonomous robotics fish," *Indian Journal of geo-Marine Science*, vol. 40, pp. 157–167, April 2011.

[2] J. L. Chew, T. B. Koay, Y. T. Tan, Y. H. Eng, R. Gao, M. Chitre, and N. Chandhavarkar, "Starfish: An open-architecture auv and its applications," in *Defense Technology Asia 2011*, Feb 2011.

[3] N. Otsu, "A threshold selection method from gray-level histograms," *Systems, Man and Cybernetics, IEEE Transactions on*, vol. 9, no. 1, pp. 62–66, 1979.

[4] I. Quidu, A. Hetet, Y. Dupas, and S. Lefevre, "Auv (redermor) obstacle detection and avoidance experimental evaluation," in *OCEANS 2007 - Europe*, June 2007, pp. 1–6.

[5] S. Zhao, T.-F. Lu, and A. Anvar, "Automatic object detection for auv navigation using imaging sonar within confined environments," in *Industrial Electronics and Applications, 2009. ICIEA 2009. 4th IEEE Conference on*, May 2009, pp. 3648 –3653.

[6] S. Zhao, T.-F. Lu, and A. Anvar, "Multiple obstacles detection using fuzzy interface system for auv navigation in natural water," in *Industrial Electronics and Applications (ICIEA), 2010 the 5th IEEE Conference on*, 2010, pp. 50 –55.

[7] H. Finn and R. Johnson, "Adaptive detection mode with threshold control as a function of spatially sampled clutter-level estimates," *RCA Review*, vol. 29, no. 3, pp. 414 – 464, 1968.

[8] P. Swerling, "Probability of detection for fluctuating targets," *Information Theory, IRE Transactions on*, vol. 6, no. 2, pp. 269–308, 1960.

[9] A. Elfes, "Using occupancy grids for mobile robot perception and navigation," *Computer*, vol. 22, no. 6, pp. 46 –57, jun 1989.

[10] S. Thrun, W. Burgard, and D. Fox, *Probabilistic Robotics*. The MIT Press, 2005.

[11] Tritech. (2013) Micron dst sector scanning sonar. [Online]. Available: http://www.tritech.co.uk/product/small-rov-mechanical-sector-scanning-sonar-tritech-micron